



Year: 2020

HDL inhibits endoplasmic reticulum stress-induced apoptosis of pancreatic -cells in vitro by activation of Smoothed

Yalcinkaya, Mustafa ; Kerksiek, Anja ; Gebert, Katrin ; Annema, Wijtske ; Sibler, Rahel ;
Radosavljevic, Silvija ; Lütjohann, Dieter ; Rohrer, Lucia ; von Eckardstein, Arnold

Abstract: Loss of pancreatic β -cell mass and function as a result of sustained ER stress is a core step in the pathogenesis of diabetes mellitus type 2. The complex control of β -cells and insulin production involves hedgehog (Hh) signaling pathways as well as cholesterol-mediated effects. In fact, data from studies in humans and animal models suggest that HDL protects against the development of diabetes through inhibition of ER stress and β -cell apoptosis. We investigated the mechanism by which HDL inhibits ER stress and apoptosis induced by thapsigargin, a sarco/ER Ca^{2+} -ATPase inhibitor, in β -cells of a rat insulinoma cell line, INS1e. We further explored effects on the Hh signaling receptor Smoothed (SMO) with pharmacologic agonists and inhibitors. Interference with sterol synthesis or efflux enhanced β -cell apoptosis and abrogated the anti-apoptotic activity of HDL. During ER stress, HDL facilitated the efflux of specific oxysterols, including 24-hydroxycholesterol (OHC). Supplementation of reconstituted HDL with 24-OHC enhanced and, in cells lacking ABCG1 or the 24-OHC synthesizing enzyme CYP46A1, restored the protective activity of HDL. Inhibition of SMO countered the beneficial effects of HDL and also LDL, and SMO agonists decreased β -cell apoptosis in the absence of ABCG1 or CYP46A1. The translocation of the SMO-activated transcription factor glioma-associated oncogene GLI-1 was inhibited by ER stress but restored by both HDL and 24-OHC. In conclusion, the protective effect of HDL to counter ER stress and β -cell death involves the transport, generation, and mobilization of oxysterols for activation of the Hh signaling receptor SMO.

DOI: <https://doi.org/10.1194/jlr.RA119000509>

Posted at the Zurich Open Repository and Archive, University of Zurich

ZORA URL: <https://doi.org/10.5167/uzh-190125>

Journal Article

Published Version

Originally published at:

Yalcinkaya, Mustafa; Kerksiek, Anja; Gebert, Katrin; Annema, Wijtske; Sibler, Rahel; Radosavljevic, Silvija; Lütjohann, Dieter; Rohrer, Lucia; von Eckardstein, Arnold (2020). HDL inhibits endoplasmic reticulum stress-induced apoptosis of pancreatic β -cells in vitro by activation of Smoothed. *Journal of Lipid Research*, 61(4):492-504.

DOI: <https://doi.org/10.1194/jlr.RA119000509>



HDL inhibits endoplasmic reticulum stress-induced apoptosis of pancreatic β -cells in vitro by activation of Smoothed^S

Mustafa Yalcinkaya,* Anja Kerkisiek,[†] Katrin Gebert,* Wijske Annema,* Rahel Sibling,*
 Silvija Radosavljevic,* Dieter Lütjohann,[†] Lucia Rohrer,* and Arnold von Eckardstein^{1,*}

Institute of Clinical Chemistry,* University and University Hospital of Zurich, Zurich, Switzerland; and
 Institute of Clinical Chemistry and Clinical Pharmacology,[†] University Hospital Bonn, Bonn, Germany

ORCID ID: 0000-0002-1666-2266 (A.v.E.)

Abstract Loss of pancreatic β -cell mass and function as a result of sustained ER stress is a core step in the pathogenesis of diabetes mellitus type 2. The complex control of β -cells and insulin production involves hedgehog (Hh) signaling pathways as well as cholesterol-mediated effects. In fact, data from studies in humans and animal models suggest that HDL protects against the development of diabetes through inhibition of ER stress and β -cell apoptosis. We investigated the mechanism by which HDL inhibits ER stress and apoptosis induced by thapsigargin, a sarco/ER Ca^{2+} -ATPase inhibitor, in β -cells of a rat insulinoma cell line, INS1e. We further explored effects on the Hh signaling receptor Smoothed (SMO) with pharmacologic agonists and inhibitors. Interference with sterol synthesis or efflux enhanced β -cell apoptosis and abrogated the anti-apoptotic activity of HDL. During ER stress, HDL facilitated the efflux of specific oxysterols, including 24-hydroxycholesterol (OHC). Supplementation of reconstituted HDL with 24-OHC enhanced and, in cells lacking ABCG1 or the 24-OHC synthesizing enzyme CYP46A1, restored the protective activity of HDL. Inhibition of SMO countered the beneficial effects of HDL and also LDL, and SMO agonists decreased β -cell apoptosis in the absence of ABCG1 or CYP46A1. The translocation of the SMO-activated transcription factor glioma-associated oncogene GLI-1 was inhibited by ER stress but restored by both HDL and 24-OHC. **In conclusion, the protective effect of HDL to counter ER stress and β -cell death involves the transport, generation, and mobilization of oxysterols for activation of the Hh signaling receptor SMO—Yalcinkaya, M., A. Kerkisiek, K. Gebert, W. Annema, R. Sibling, S. Radosavljevic, D. Lütjohann, L. Rohrer, and A. von Eckardstein. HDL inhibits endoplasmic reticulum stress-induced apoptosis of**

pancreatic β -cells in vitro by activation of Smoothed. *J. Lipid Res.* 2020. 61: 492–504.

Supplementary key words adenosine 5'-triphosphate binding cassette transporter • cytochrome P450 enzyme • high density lipoprotein • cholesterol efflux • cholesterol metabolism • oxysterols • lipoprotein receptors • hedgehog signaling

Loss of pancreatic β -cell mass and function is the ultimate step in the pathogenesis of diabetes mellitus type 2 (1). Disturbed insulin secretion, high concentrations of glucose or FFAs, and other factors can lead to ER stress and, as the consequence, β -cell apoptosis (2–5). ER stress is a protective mechanism involving chaperones to assist refolding and degradation of unfolded proteins. In the case of sustained and extreme ER stress, the apoptotic mediator C/EBP homologous protein (CHOP) promotes cell death by decreasing B-cell lymphoma (Bcl)-2 expression (2, 6).

HDLs promote the survival of different cell types. In pancreatic β -cells, HDL inhibits pro-apoptotic effects of native and oxidized LDLs, interleukin (IL)-1 β , FFAs, tunicamycin, or thapsigargin (TG) (7). The underlying mechanisms and receptors are unknown. However, they could help to explain the inverse association between plasma HDL-cholesterol and the risk of incident diabetes, which was observed in both epidemiological and genetic studies (8, 9) as well as the opposite modulation of glucose tolerance in

This work was supported by a Sinergia grant from the Swiss National Science Foundation (SNF, CRSII3_154420), a Systems X Program Grant MRD 2014/267, and a grant from the Swiss Heart Foundation to A.v.E. R.S. was supported by Forschungskredit of Universität Zürich. W.A. was supported by funding from the Ter Meulen Fund, Royal Netherlands Academy of Arts and Sciences. The authors declare that they have no conflicts of interest with the contents of this article.

Manuscript received 31 October 2019 and in revised form 18 December 2019.

Published, JLR Papers in Press, January 6, 2020
 DOI <https://doi.org/10.1194/jlr.RA119000509>

Abbreviations: CHOP, C/EBP homologous protein; CYP, cytochrome P450; DHCR24, 24 dehydrocholesterol reductase; DOPC, dioleoyl phosphatidylcholine; For, forward; GLI-1, glioma-associated oncogene; Hh, hedgehog; Ihh, Indian hedgehog; OHC, hydroxycholesterol; Ptch1, Patched 1; Rev, reverse; rHDL, reconstituted HDL; SAG, Smoothed agonist; Smo, Smoothed; *Scarb1*/SR-BI, scavenger receptor BI; TBP, TATA-binding protein; TG, thapsigargin.

¹To whom correspondence should be addressed.

e-mail: arnold.voneckardstein@usz.ch

^S The online version of this article (available at <https://www.jlr.org>) contains a supplement.

Copyright © 2020 Yalcinkaya et al. Published under exclusive license by The American Society for Biochemistry and Molecular Biology, Inc.
 This article is available online at <https://www.jlr.org>

genetic mouse models with HDL deficiency versus high HDL-cholesterol (10).

Cellular effects of HDL have been explained by two principal concepts. One model highlights direct and specific interactions between HDL-bound agonists and cellular receptors (11, 12). The other model emphasizes the importance of HDL-induced cholesterol efflux via ABCA1 and ABCG1, which primarily alter cellular cholesterol homeostasis and, secondarily, cell function and survival (11, 13). The quantity of cellular cholesterol determines the activity of transcription factors, such as SREBPs and LXRs (14). The crucial role of both SREBP2 and LXRs as well as their most prominent target genes, namely the LDL receptor and the mentioned ABC transporters, respectively, for β -cell function and hence glucose homeostasis have been demonstrated in β -cell-specific knockout mice (15–18). Alterations in the subcellular distribution of cholesterol also modulate the activity of membrane-bound proteins. A recently elaborated example is the interaction of the hedgehog (Hh) signaling molecules Smoothened (SMO) and Patched 1 (PTCH1): Depending on the distribution of cholesterol between the inner and outer leaflets of the plasma membrane, either SMO or its inhibitor PTCH1 is more active (19). Hh signaling plays an important role in pancreas development as well as regulation of insulin production and cytokine-induced apoptosis of β -cells (20, 21).

In the present study, we aimed to unravel the mechanism by which native HDL as well as mimetics of HDL, such as CSL-111, which was previously found to improve glycemia in diabetic patients (22), inhibit ER stress and subsequent apoptosis of pancreatic β -cells induced by TG, which is a sarco/ER Ca^{2+} -ATPase inhibitor that induces ER calcium depletion (23, 24). By using the rat insulinoma cell line INS1e, we show that the cytoprotective effect of HDL in β -cells involves the generation and efflux of specific oxysterols by cytochrome P450 (CYP) enzymes and ABC transporters, respectively, and the subsequent activation of SMO by these oxysterols to elicit the nuclear translocation of its downstream target, namely, glioma-associated oncogene (GLI-1), a member of the zinc-finger protein family (25).

MATERIALS AND METHODS

Cell culture

Rat pancreatic β -cell line INS1es (26), generated and provided by Prof. C. Wollheim (27), were cultured in RPMI-1640 medium (R8758-500ML, Sigma-Aldrich, St. Louis, USA) with 5% fetal bovine serum (F7524, Sigma-Aldrich), 100U/ml of penicillin and 100ug/ml streptomycin (P0781, Sigma-Aldrich), 1 mM Sodium Pyruvate (S8636-100ML, Sigma-Aldrich), 10 mM HEPES Buffer (H0887, Sigma-Aldrich) and 0.0004% 2-Mercaptoethanol (Fluka 63689, Fluka, Steinheim, Germany) at 37°C in a humidified 5% CO_2 , 95% air incubator.

Isolation of LDL and HDL and preparation of reconstituted HDL

LDL ($1.006 < d < 1.063$ g/ml) and HDL ($1.063 < d < 1.21$ g/ml) were isolated from fresh human plasma of normolipidemic blood

donors by sequential ultracentrifugation as described previously (28, 29). ApoA-I was isolated from HDL by fast-performance LC (FPLC) (30). For functional validation of our candidate lipids, reconstituted HDLs (rHDLs) were produced by the use of the cholate dialysis method (31, 32). rHDLs consist of apoA-I and dioleoyl phosphatidylcholine (DOPC; 850375; Avanti Polar Lipids) in a molar ratio of 1:100 with or without the sterol of interest. The 7α -hydroxycholesterol (OHC) (Avanti Polar Lipids; 700034), 7β -OHC (Avanti Polar Lipids; 700035), 24(R,S)-OHC (Sigma; #SML1648), or 25-OHC (Avanti Polar Lipids; 700019) were included at two different molar ratios relative to apoA-I, namely, 0.01 and 0.001, which mimic the lower and upper concentration range of oxysterols in HDL. Cholesterol (Sigma; C8667) was included at three different molar ratios relative to apoA-I, which either reflect the situation in native HDL (10) or mimic the concentrations of oxysterols (0.01 and 0.001). CSL-111, was kindly provided by CSL Behring (King of Prussia, PA). This HDL mimetic contains an apoA-I-rich plasma protein fraction and phosphatidylcholine derived from soybean. It is the prototype version of CSL-112 developed for the treatment of atherosclerotic cardiovascular disease (33, 34). Interestingly, infusion of CSL-111 was previously shown to improve glycemia in patients with diabetes (22).

siRNA transfection

Abca1 (M-092371-01-0005), *Smo* (L-089918-02-0005), *Ptch1* (L-095232-02-0005), Indian Hh (*Ihh*) (L-084006-02-0005), *Cyp46a1* (L-10000-02-0010), and *Ch25h* (#L-085924-02-0010) were silenced by forward transfection with Dharmacon ON-TARGETplus siRNA oligonucleotides (Dharmacon, Lafayette, CO). D-001810-10-05 was used as the nonsilencing control. Microsynth siRNA oligonucleotides were used to target scavenger receptor BI (*Scarb1*) (5'-GCA GCA GGU GCU CAA GAA U dTdT-3') and *Abcg1* (5'-UGA AUA UUC UGG CGG GAU A dTdT-3') with 5'-AGA GCU UAU CCC UCG GUU GUG UCG U dTdT-3' as the nonsilencing control. Ambion Silencer Select and Life Technologies siRNA oligonucleotides were used to target 24 dehydrocholesterol reductase (*Dhcr24*) (s151265) and nonsilencing control (4390843). All siRNAs were used at a final concentration of 20 nmol/l using Lipofectamine RNAiMAX transfection reagent (13778150; Invitrogen, Carlsbad, CA) in an antibiotic-free medium according to the manufacturers' instructions. The efficiency of knockdowns was determined by Western blot or real-time PCR using TATA-binding protein (TBP) and *Rn18s* expression levels as loading control and references, respectively.

Real-time PCR

Real-time PCR was performed on a Roche Light Cycler 480-II (05015243001; Roche, Switzerland). RNA was extracted using Tri-reagent (T9424; Sigma-Aldrich) according to manufacturer's instructions, and cDNA was generated using the RevertAid First Strand synthesis kit (K1621; Thermo Fischer Scientific). Real-time PCR reactions were performed using the LightCycler® 480 SYBR Green I Master (04887352001; Roche, Mannheim, Germany) using gene-specific primers as follows: *Chop* [forward (For): TTC ACT ACT CTT GAC CCT GCA TCA GTG CGC CTT CAC TTT GG; reverse (Rev): CAC TGA CCA CTC TGT TTC CGT TTC], *Atf4* (For: CAT GGG TTC TCC AGC GAC AA; Rev: CGT GGC CAA AAG CTC ATC TG), *Xbp1* spliced (For: TGC TGA GTC CGC AGC AGG TG; Rev: ATT AGC AGA CTC TGG GGA AG), *Dhcr24* (For: GCT GCA CAC CGT CTG AAA AC; Rev: TTC TTG GCA GGG ATG ATG CG), *Cyp46a1* (For: AGA CTT CCG GCA ACC ATC TG; Rev: CCC CAG ATC CTC GTA GTC CA), *Ch25h* (For: GGA CAG CAT AAG GAC GGG AG; Rev: ACA TCT AGC ACC ACG AAC GG), *Smo* (For: ATG CGT GTT TCT TTG TGG GC; Rev: ACA CAG GAT AGG GTC TCG CT), *Ptch1* (For: CGT TCT

CAC AAC CCT CGG AA; Rev: TCT CGG GGT AGC TCT CGT AG), *Ihh* (For: GGA CCC CAA GTG AAG GTG TT; Rev: AGG AGG GCA GTG GTT AGA GT), normalized to *Rn18s* (For: GCT GAG AAG ACG GTC GAA CT; Rev: TTA ATG ATC CTT CCG CAG GT).

Apoptosis assays

INS1e cells were plated in 96-well plates (2.5×10^4 cells per well) for the free nucleosome assay and in 24-well plates (2×10^5 cells per well) for the caspase-3 activity assay. Cells were cultured for 2 days and treated with 100 nM and 50 nM TG (T9033; Sigma-Aldrich) for 4 and 16 h, respectively, in the presence or absence of 50 μ g/ml native HDL, 25 μ g/ml CSL-111, or 20 μ g/ml rHDL. Cell death was recorded by measuring free nucleosomes with the Cell Death ELISA (#11920685001; Roche) and Caspase-3 Fluorimetric Assay kit (#CASP3F; Sigma). For fluorescence-activated cell sorting (FACS) experiments, cells were detached with Accutase (A6964; Sigma-Aldrich) and resuspended in FACS buffer containing 0.01 M HEPES (pH 7.4), 0.14 M NaCl, and 2.5 mM CaCl_2 at the end of the incubation period. Then, cells were stained with annexin V labeled with Alexa-Fluor 647 (BioLegend, San Diego CA) and propidium iodide (US Biological, Swampscott, MA) and analyzed in a CyAn ADP flow cytometer (Beckman-Coulter, Brea CA). Data were analyzed using Flowing Software version 2. Early apoptotic cells were defined as Annexin V positive and propidium iodide negative and late apoptotic cell were defined as annexin V-positive and propidium iodide-positive. Where indicated, cells were pretreated for 30 min at 37°C with 20 μ M cyclopamine (#1623; Tocris, Bristol, UK) following TG and HDL treatment or with 1 μ M or 200 nM 2(S)-OHC (#4474; Tocris), 10 or 20 nM Smo agonist (SAG) dihydrochloride (#6390; Tocris) in the presence of TG for 4 h.

Measurement of sterols

Cholesterol, noncholesterol sterols and oxysterols were quantified in both cells and media. The trimethylsilylated sterol and di-trimethylsilylated oxysterol ethers were separated by gas chromatography (GC). Cholesterol was detected by less sensitive but specific flame-ionization detection (FID) (5 α -cholestane, internal standard, ISTD), the noncholesterol sterols (epicoprostanol, ISTD) and the oxysterols ($^2\text{H}_x$ -oxysterols, ISTD) by highly specific and highly sensitive mass spectrometry in the selected ion monitoring mode (MS-SIM) as described in detail previously (35, 36).

Western blotting

INS1e cells were lysed in RIPA buffer [10 mmol/l Tris (pH 7.4), 150 mmol/l NaCl, 1% NP-40, 1% sodium deoxycholate, 0.1% SDS, and protease inhibitors (11836153001; Roche)]. For fractionation, INS1e cells (5 million cells seeded on a 10 cm plate and followed by the same treatment as described before) were lysed in 500 μ l of fractionation buffer [20 mM HEPES (pH 7.4), 10 mM KCl, 2 mM MgCl_2 , 1 mM EDTA, 1 mM EGTA, 1 mM DTT, and protease inhibitors (11836153001; Roche)] and incubated for 15 min on ice. After that, lysates were passed through a 27 gauge needle 10 times and left on ice for 20 min. The lysates were centrifuged at 720 g for 5 min. The supernatants were stored as cytoplasmic fraction. Nuclear pellets were washed with 500 μ l of fractionation buffer and passed through a 25 gauge needle 10 times. They were centrifuged again at 720 g for 10 min and the pellet was stored as a nuclear fraction. Equal amounts of protein were separated on SDS-PAGE and trans-blotted onto PVDF membrane (10600023; GE Healthcare, Munich, Germany). Membranes were blocked in appropriate blocking buffer recommended for

the antibody (PBS-T supplemented with 5% milk or BSA) and incubated overnight on a shaker at 4°C with primary antibodies at a dilution of 1:1,000 in the same blocking buffer. Membranes were incubated for 1 h with HRP-conjugated secondary antibody (Dako) in blocking buffer at a dilution of 1:2,500. Membranes were further incubated with chemiluminescence substrate for 1 min (34577; Thermo Scientific) and imaged using Fusion Fx (Vilber, Marne-la-Vallée, France). Antibodies were used for immunodetection of ABCA1 (ab18180, Abcam, Cambridge, UK), ABCG1 (ab52617, Abcam), SR-BI (NB400-131, Novus Biologicals, Centennial, CO) and GLI-1 (2534S, Cell Signalling Technology, Leiden, The Netherlands), TBP (ab51841, Abcam), or α -Tubulin (T9026, Sigma).

Statistical analysis

The data sets for all validation experiments were analyzed using the GraphPad Prism 8 software. Comparison between groups was performed using one-way ANOVA coupled with Tukey's test for multiple comparisons. The data were obtained from at least three independent experiments, performed in triplicates or quadruplets. Values are expressed as mean \pm SD. $P < 0.05$ was regarded as significant.

RESULTS

HDL protects INS1e cells from TG-induced cell death and ER-stress

We tested the ability of HDL to inhibit the apoptosis of INS1e cells as induced by TG that was previously shown to induce ER stress and apoptosis in mouse insulinoma 6 (Min6) cells and human islets (7, 23). INS1e cells were stimulated with 50 nM of TG to induce ER stress-dependent apoptosis and incubated with increasing dosages of native HDL for 16 h. TG-induced apoptosis was reduced dose dependently by HDL; half-maximal inhibition was recorded at a concentration of 50 μ g/ml HDL (supplemental Fig. S1A–D). The cells were treated with 100 nM or 50 nM of TG for 4 or 16 h in the presence or absence of 50 μ g/ml native HDL or 25 μ g/ml CSL-111, an artificial rHDL, which contains an apoA-I-rich human plasma protein fraction and soybean phosphatidylcholine, which mimics several functions of physiological HDL (33) and which was previously found to improve glycemia (22). For either time point, both HDL and CSL-111 reduced the apoptosis of INS1e cells, independently of whether apoptosis was recorded as free nucleosomes or caspase-3 activity (Fig. 1A–D). Interestingly, lipid-free apoA-I did not inhibit TG-induced apoptosis (supplemental Fig. S2).

HDL inhibited the various components of ER stress by different time kinetics: During 4 h incubation, TG increased *Xbp1* splicing as well as the expression of *Atf4* and *Chop*. HDL and CSL-111 abrogated *Xbp1* splicing but had either no effect (HDL) or increasing effects (CSL-111) on the expression of *Atf4* and *Chop* (Fig. 2A–C). By contrast, during the 16 h incubation with INS1e cells, TG did not alter *Xbp1* splicing but increased the expression of *Atf4* and *Chop*, and this effect was mitigated by both HDL and CSL-111 (Fig. 2D–F). Taken together, HDL and CSL-111 inhibit ER stress of INS1e cells.

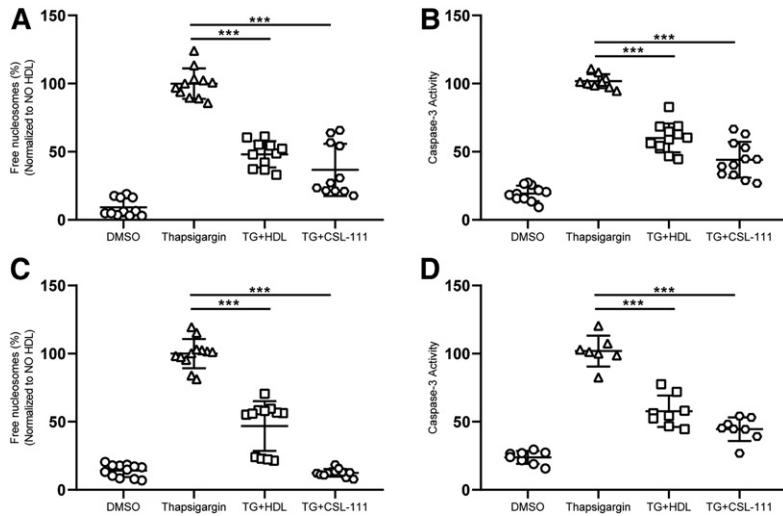


Fig. 1. Short- and long-term effects of HDL and CSL-111 on cell death. INS1e cells were treated with 100 nM or 50 nM of TG for 4 h (A, B) or 16 h (C, D) in the presence or absence of 50 or 25 μ g/ml native HDL or CSL-111. Cell death was recorded by measuring free nucleosomes (A, C) or caspase-3 activity (B, D). Data are presented as the mean \pm SD of three independent experiments, which were analyzed by one-way ANOVA coupled with Tukey's test for multiple comparisons. *** $P \leq 0.001$, ** $P \leq 0.01$, * $P \leq 0.05$.

HDL anti-apoptotic activity is related to cellular cholesterol homeostasis

We next investigated the contribution of cholesterol homeostasis to the protective effects of HDL. To this end, we interfered with either the synthesis or the efflux of cholesterol. Potential candidates (*Dhcr14*, *Abca1*, and *Abcg1* as well as *Scarb1*) were silenced with siRNA transfection. Knockdown of the candidates was 70% for *Dhcr24*, 95% for ABCA1 and ABCG1, and 75% for SR-BI (supplemental Figs. S3A, S4). Forty-eight hours after transfection, the cells were treated with TG for 4 h in the presence or absence of HDL or CSL-111. The knockdown of *Dhcr24*, encoding the last enzyme of the cholesterol synthesis pathway, escalated

TG-induced cell death and abolished the anti-apoptotic activities of both HDL and CSL-111 (supplemental Fig. S3B). Likewise, the pharmacological inhibition of cholesterol synthesis by mevastatin reduced the anti-apoptotic activities of HDL and CSL-111 (supplemental Fig. S3C). Knockdown of *Abcg1* and *Abca1*, but not *Scarb1*, increased TG-induced cell death 3-fold and abolished or mitigated the anti-apoptotic activities of HDL and CSL-111 (Fig. 3A–C).

Sterols are differentially effluxed by HDL from INS1e cells

Apparently, the anti-apoptotic activity of HDL and CSL-111 depends on the presence and mobilization of cholesterol or its derivatives. To unravel any specific sterols

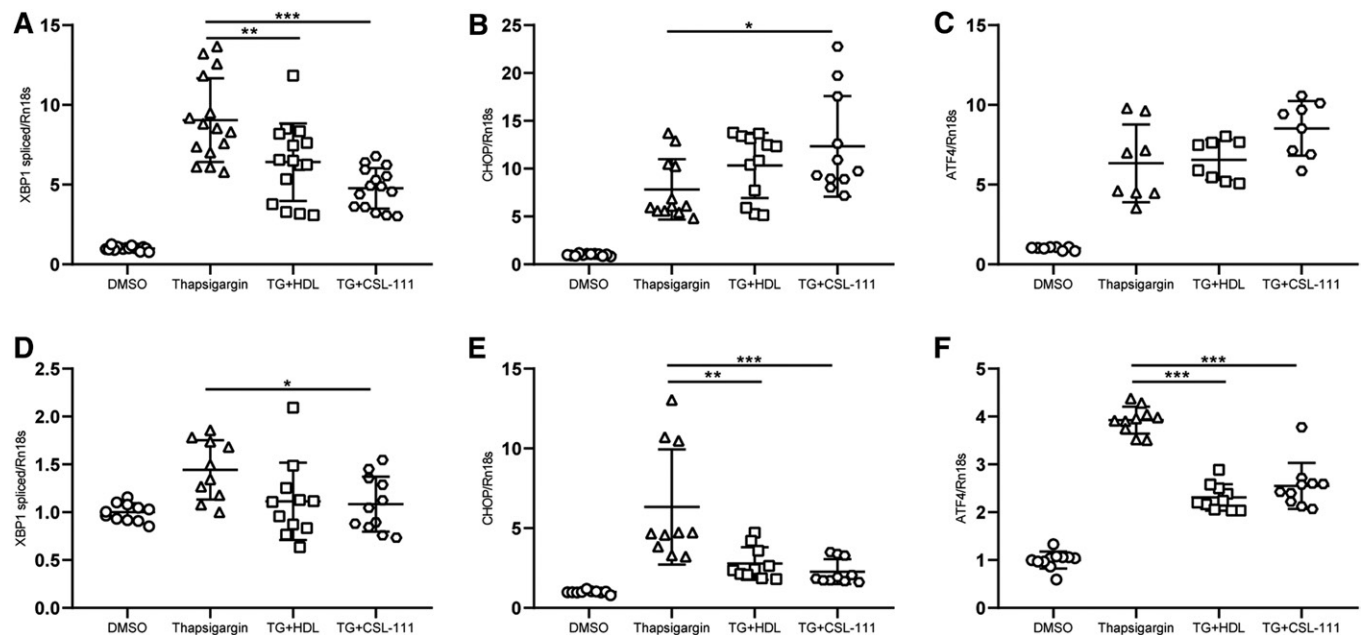


Fig. 2. Short- and long-term effects of HDL and CSL-111 on ER stress. INS1e cells were treated with 100 nM or 50 nM of TG for 4 h (A–C) or 16 h (D–F) in the presence or absence of 50 or 25 μ g/ml native HDL or CSL-111. ER stress-responsive gene expression was measured by quantitative PCR. *Xbp1* splicing (A, D), *Chop* expression (B, E), and *Atf4* expression (C, F). Data are presented as the mean \pm SD of three independent experiments, which were analyzed by one-way ANOVA coupled with Tukey's test for multiple comparisons. *** $P \leq 0.001$, ** $P \leq 0.01$, * $P \leq 0.05$.

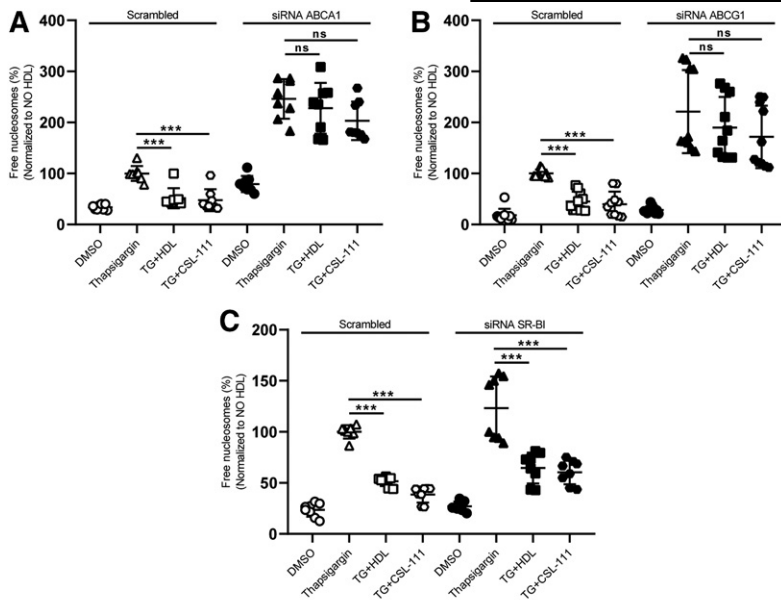


Fig. 3. The anti-apoptotic activity of HDL depends on ABCA1- and ABCG1-dependent cholesterol efflux. INS1e cells were transfected with specific siRNA against *Abca1* (A), *Abcg1* (B), *Scarb1* (C), or with nonsilencing siRNA (Scrambled). After 48 h of transfection, the cells were treated with 100 nM of TG and incubated with native HDL or CSL-111 for 4 h. Cell death was recorded by the use of the free nucleosomes assay. Data are presented as the mean \pm SD of three independent experiments, which were analyzed by one-way ANOVA coupled with Tukey's test for multiple comparisons in groups of Scrambled and knockdown conditions, respectively. *** $P \leq 0.001$, ** $P \leq 0.01$, * $P \leq 0.05$.

produced and released by INS1e cells in response to TG and/or HDL, we incubated INS1e cells with CSL-111 for 16 h. We collected media and cell pellets for the measurement of sterols by GC-MS. In both the presence and absence of TG, CSL-111 significantly increased the amount of 7 α -OHC, 7 β -OHC, 24-OHC, and 25-OHC in cell culture media (Fig. 4F–I) and decreased the cellular content in 7 β -OHC and 24-OHC (supplemental Fig. S5G, H). However, CSL-111 promoted net cholesterol efflux into the medium only in the absence of TG (Fig. 4D). Cellular desmosterol, cholesterol, and cholestanol were also dimin-

ished by CSL-111 treatment both in the presence and absence of TG (supplemental Fig. S5C–E). In the presence of CSL-111, the amounts of lanosterol and lathosterol increased in both cellular and extracellular fractions (Fig. 4A, B; supplemental Fig. S5A, B). Altogether, these results show that HDL preferentially facilitates efflux of oxysterols from INS1e cells under ER stress.

The anti-apoptotic activity of HDL depends on oxysterols

We next examined whether supplementation with oxysterols or cholesterol improves the anti-apoptotic activities

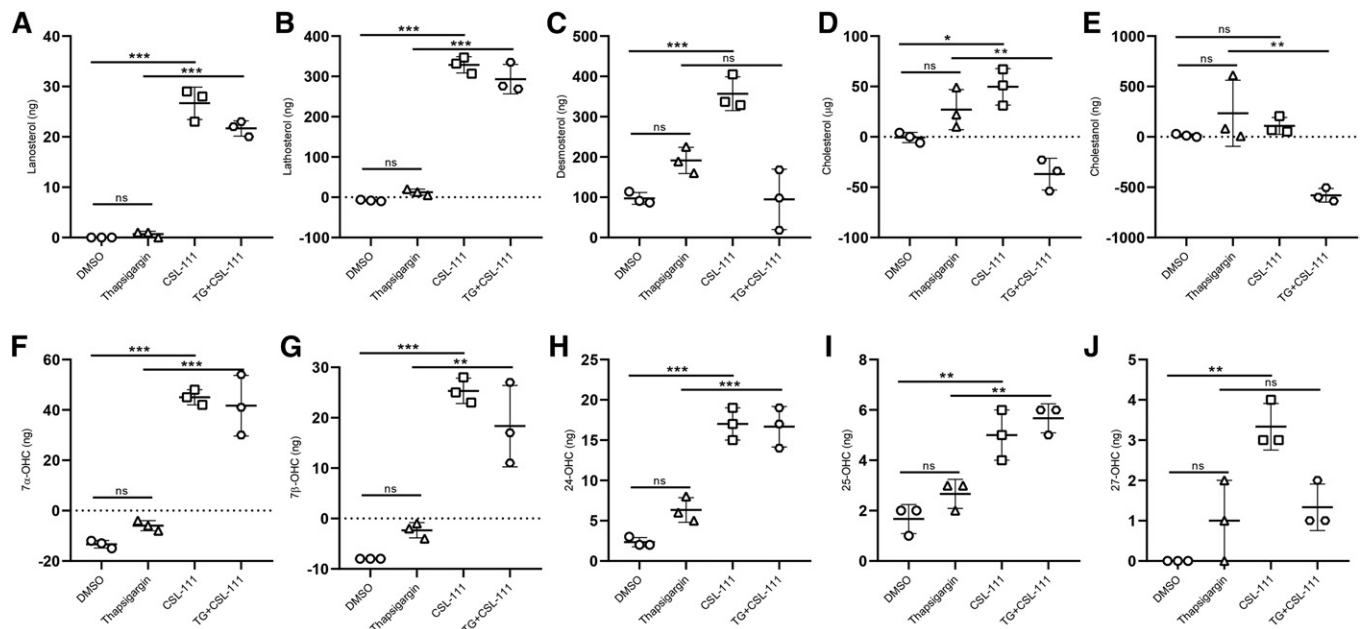


Fig. 4. Sterols are differentially effluxed by HDL from INS1e cells. INS1e cells were treated with 50 nM of TG in the presence or absence of CSL-111 for 16 h, and sterols were measured by mass spectrometry from cell medium. Starting sterol amounts were subtracted from amounts measured after 16 h for each condition separately. Lanosterol (A), lathosterol (B), desmosterol (C), cholesterol (D), cholestanol (E), 7 α -OHC (F), 7 β -OHC (G), 24-OHC (H), 25-OHC (I), and 27-OHC (J). Data are presented as the mean \pm SD and were analyzed by one-way ANOVA coupled with Tukey's test for multiple comparisons. *** $P \leq 0.001$, ** $P \leq 0.01$, * $P \leq 0.05$.

of initially sterol-free rHDL. We used the cholate dialysis method to generate rHDL consisting of apoA-I and DOPC in a molar ratio of 1:100 with or without the sterol of interest. The respective candidate sterols are included in rHDL at different amounts, which reflects their physiological concentrations in native HDL. Addition of very low amounts of 24-OHC and 25-OHC improved rHDL's anti-apoptotic activities (Fig. 5). The same was observed for cholesterol (Fig. 5). Interestingly, supplementation of rHDL with 7 α -OHC and 7 β -OHC did not improve the anti-apoptotic activity of rHDL (supplemental Fig. S6).

Oxysterols are produced from cholesterol, either by enzymes of the CYP superfamily or by reactive oxygen species. INS1e cells express 24-OHC producing cholesterol 24-hydroxylase (*Cyp46a1*) strongly, the 25-OHC generating cholesterol 25-hydroxylase (*Ch25h*) to little extent, and the 7 α -OHC generating cholesterol 7 α -hydroxylase (*Cyp7a1*) at very low amounts. We therefore focused the RNA interference experiments on *Cyp46a1* and *Ch25h*. Knockdown efficiency of *Cyp46a1* and *Ch25h* was 71% and 85%, respectively (supplemental Fig. S7). Forty-eight hours after siRNA transfection, the cells were incubated with TG for 4 h in the presence or absence of HDL or rHDL. Both silencing of *Cyp46a1* and *Ch25h* boosted TG-induced β -cell death (Fig. 6A, B). The survival-promoting effect of native HDL was completely abolished under either condition, whereas rHDL was able to reduce apoptosis upon *Ch25h* knockdown but not *Cyp46a1* knockdown (Fig. 6A, B).

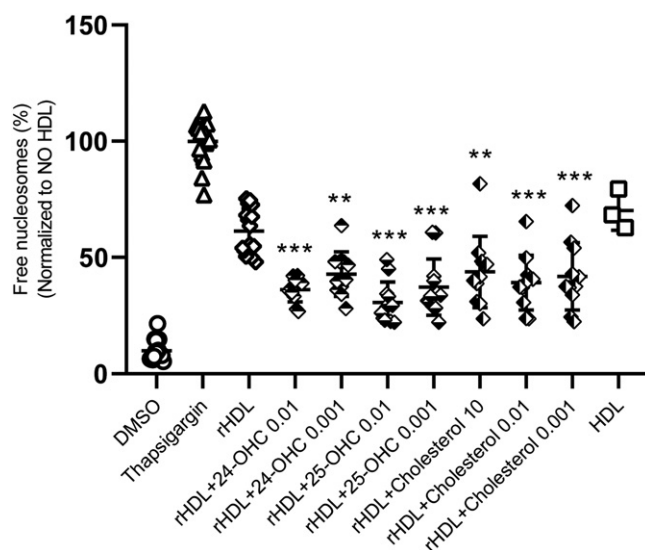


Fig. 5. Supplementation with 24-OHC, 25-OHC, or cholesterol enhances apoptosis inhibition by rHDL. rHDLs were supplemented with the indicated oxysterols at two different molar ratios relative to apoA-I, namely 0.01 and 0.001, representing the concentration range observed in the efflux experiment described in Fig. 4. Cholesterol was added at three different molar ratios relative to apoA-I, namely 10 representing the situation in native HDL as well as 0.01 and 0.001 like the oxysterols. INS1e cells were treated with 100 nM of TG and incubated with 20 μ g/ml rHDL^{-/+} oxysterols for 4 h. Cell death was recorded via free nucleosomes assay. Data are presented as mean \pm SD of 3 independent experiments and analyzed by one-way ANOVA coupled with Tukey's test for multiple comparisons of rHDL \pm oxysterols against rHDL. *** $P \leq 0.001$, ** $P \leq 0.01$, * $P \leq 0.05$.

Taken together, the data indicate the importance of oxysterols, either produced endogenously by the cells or provided exogenously with HDL, for the anti-apoptotic activity of HDL toward INS1e cells.

We next investigated to determine whether supplementation with oxysterols can restore the ability of rHDL to prevent β -cell death of cells in which oxysterol generation and efflux were compromised by the knockdown of *Cyp46a1*, *Ch25h*, or *Abcg1*, respectively. As shown before for HDL and CSL-111 (Figs. 3B, 6A), the knockdown of either *Cyp46a1*, *Ch25h*, or *Abcg1* increased the apoptotic effect of TG and dramatically decreased the anti-apoptotic effect of rHDL (Fig. 7A–C, respectively). The addition of 24-OHC, 25-OHC, or cholesterol completely rescued the anti-apoptotic activity of rHDL in the absence of *Abcg1* (Fig. 7C) or *Ch25h* (Fig. 7B) but only to a lesser extent in the absence of *Cyp46a1* (Fig. 7A). Because oxysterols can activate LXR, we wondered whether the synthetic LXR agonist, T0901317, could prevent the increase in cell death elicited by silencing of *Cyp46a1* or *Ch25h*. Pretreatment of INS1e cells with LXR agonist T0901317 did not change cell death under basal or ER stress conditions (supplemental Fig. S8).

Altogether, our data show that the anti-apoptotic activity of HDL requires the mobilization of specific oxysterols by ABCG1 or ABCA1.

HDL anti-apoptotic activity depends on Hh signaling

Hh signaling was previously shown to protect INS1e cells from cytokine-induced cell death (20). Moreover, cholesterol and oxysterols are known to regulate the activity of SMO, either by modulating the interaction with its inhibitor, PTCH1, or by direct activation (19, 37). Therefore, we investigated the contribution of Hh signaling to the anti-apoptotic function of HDL. In a first step, we silenced key players of Hh signaling with siRNAs against *Ptch1*, *Smo*, and *Ihh* prior to TG treatment. The knockdown efficiencies were 82% for *Smo*, 70% for *Ptch1*, and 72% for *Ihh* (supplemental Fig. S9). Forty-eight hours after transfection, the cells were treated with TG for 4 or 16 h in the presence or absence of HDL or CSL-111. The anti-apoptotic effect of both native HDL and CSL-111 was significantly blunted by the RNA interference with *Smo* (Fig. 8A, supplemental Fig. S10A) but not by interference with *Ptch1* or *Ihh* (supplemental Fig. S11A–D). We further tested the contribution of SMO to the anti-apoptotic activity of HDL by pharmacological inhibition. Preincubation of INS1e cells with the SMO inhibitor, cyclopamine, for 30 min significantly abrogated the inhibitory effects of both HDL and CSL-111 on the appearance of free nucleosomes, i.e., markers of apoptosis (Fig. 8B) as well as *Chop* and *Atf4* expression, i.e., markers of ER stress (Fig. 8C, D) elicited by 16 h TG treatment. Also, in combination with 4 h TG treatment, SMO inhibition via siRNA knockdown (supplemental Fig. S10A) or cyclopamine treatment abrogated the inhibitory effect of HDL on apoptosis, as recorded by the free nucleosome assay (supplemental Fig. S10B) or caspase-3 activation (supplemental Fig. S10C) and on ER stress, as recorded by *Xbp1* splicing (supplemental Fig.

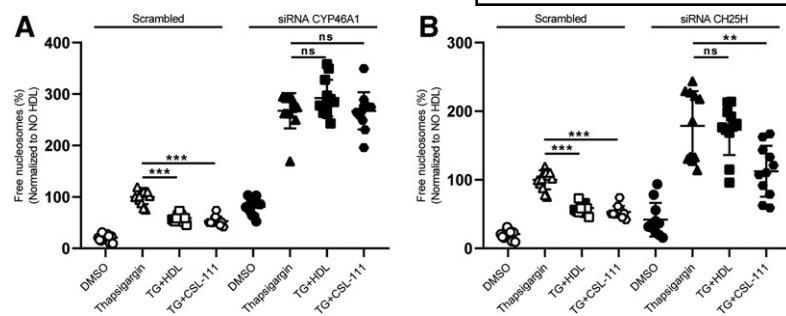


Fig. 6. Interference with oxysterol synthesizing CYP enzymes prevents inhibition of β -cell apoptosis by HDL. INS1e cells were transfected with specific siRNA against *Cyp46a1* (A), *Ch25h* (B), or with nonsilencing siRNA (Scrambled). After 48 h of transfection, the cells were treated with 100 nM of TG and incubated with HDL or CSL-111 for 4 h. Cell death was recorded by using the free nucleosomes assay (A, B). Data are represented as the mean \pm SD of three independent experiments, which were analyzed by one-way ANOVA coupled with Tukey's test for multiple comparisons in groups of Scrambled and knockdown conditions, respectively. *** $P \leq 0.001$, ** $P \leq 0.01$, * $P \leq 0.05$.

S10D). Of note, SMO inhibition further increased β -cell death (supplemental Fig. S10A–C).

Interestingly, like HDL, the synthetic 20(S)-OHC and SAG decreased TG-induced apoptosis (Fig. 9A and B, respectively) and both 20(S)-OHC and SAG rescued *Cyp46a1*- or *Abcg1*-induced β -cell death (Fig. 9C, D).

Activated SMO elicits its downstream signals by inducing the translocation of the mature transcription factor GLI-1 from the tip of the cilium into the nucleus (25). We therefore investigated to determine whether TG, HDL, and oxysterols modulate Hh signaling. INS1e cells were treated with 100 nM of TG and incubated with native HDL or rHDL in the absence or presence of sterols (24-OHC, 25-OHC, and cholesterol) for 4 h. Cells were fractionated into cytoplasmic and nuclear fractions and the fractions were immunoblotted with anti-GLI1, anti-TBP, and anti- α -tubulin. TG treatment decreased the nuclear abundance of GLI-1. Interestingly, native HDL as well as rHDL supplemented with oxysterols but not sterol-free rHDL restored the abundance of GLI-1 in the nucleus (Fig. 10A and B, respectively).

LDLs contain oxysterols as well (38, 39). Therefore, we tested to determine whether LDL had similar anti-apoptotic effects in our model. We treated the cells with 25 μ g/ml HDL or LDL or both. LDL reduced apoptosis as much as

HDL. The combined treatment with LDL and HDL further increased the anti-apoptotic activity (Fig. 11A). The oxysterol levels of the two preparations of HDL and LDL used in these experiments are shown in supplemental Table S1. Standardized per milligram of protein, LDL contains nearly 3-fold more 24-OHC and nearly 9-fold more 25-OHC than HDL. Finally, we investigated to determine whether the anti-apoptotic effect of LDL also depends on Hh signaling. SMO inhibition via siRNA knockdown (Fig. 11B) or cyclopamine treatment for 4 h (Fig. 11C) and 16 h (Fig. 11D) abrogated the inhibitory effects of both HDL and LDL.

DISCUSSION

We here investigated the mechanism by which HDL protects pancreatic β -cells from TG-induced ER stress and apoptosis. By integrating data from lipidomics and targeted experiments using RNA interference or pharmacological agents, we found a complex mechanism that involves the generation and mobilization of oxysterols by specific CYP enzymes and ABC transporters, respectively, and the sterol-mediated activation of the Hh signaling receptor SMO (Fig. 12).

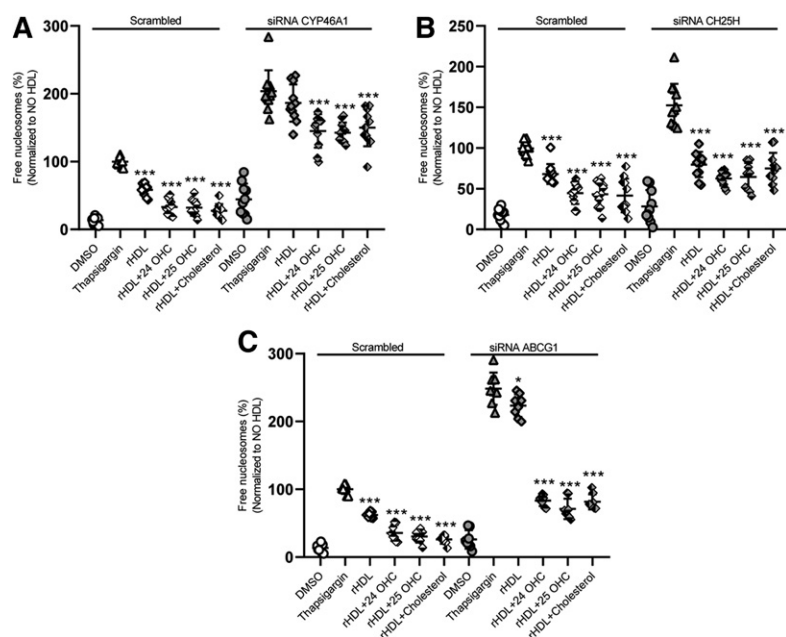


Fig. 7. Oxysterol supplementation rescues β -cell death induced by lack of CYP46A1, CH25H, or ABCG1. INS1e cells were transfected with specific siRNA against *Cyp46a1* (A), *Ch25h* (B), *Abcg1* (C), or with nonsilencing siRNA (Scrambled). After 48 h of transfection, the cells were treated with 100 nM of TG and incubated with rHDL \pm 24-OHC, 25-OHC, or cholesterol for 4 h. Cell death was recorded by the use of the free nucleosomes assay. Data are represented as the mean \pm SD of three independent experiments, which were analyzed by one-way ANOVA coupled with Tukey's test for multiple comparisons in groups of Scrambled and knockdown conditions, respectively. *** $P \leq 0.001$, ** $P \leq 0.01$, * $P \leq 0.05$.

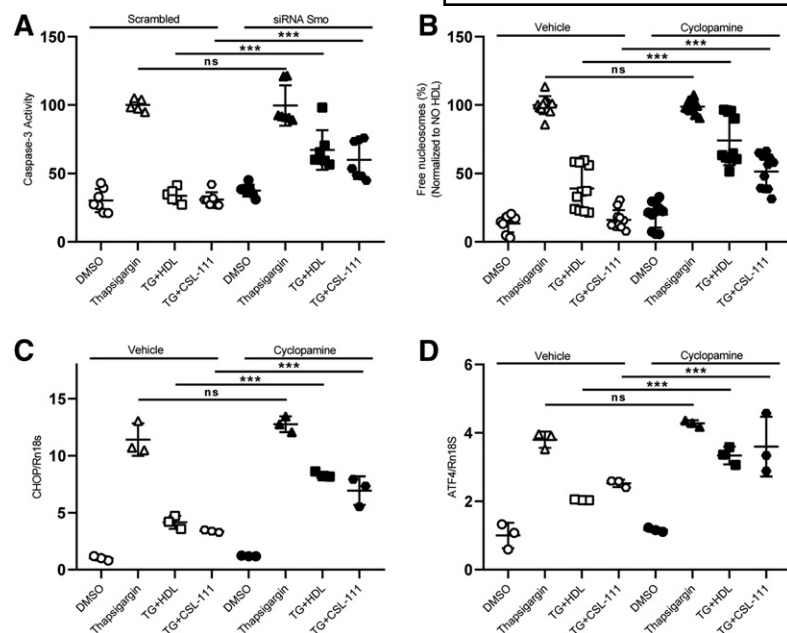


Fig. 8. Anti-apoptotic effects of HDL depend on SMO. INS1e cells were transfected with specific siRNA against *Smo* and nonsilencing siRNA (Scrambled) (A) or pretreated with cyclopamine for 30 min (B–D). After 48 h of transfection or cyclopamine treatment, the cells were treated with 50 nM of TG and incubated with HDL or CSL-111 for 16 h. *Chop* (C) and *Atf4* (D) expressions were measured by quantitative PCR. Cell death was recorded with the free nucleosomes assay (A, B). Data are presented as the mean \pm SD of three independent experiments, which were analyzed by one-way ANOVA coupled with Tukey's test for multiple comparisons. *** $P \leq 0.001$, ** $P \leq 0.01$, * $P \leq 0.05$.

Several previous observations highlight the importance of cellular cholesterol homeostasis in β -cells for the control of glucose levels in blood and hence protection against diabetes. LDL-cholesterol lowering with statins as well as low activity alleles of the *HMGCR* and *PCSK9* genes were reported to increase the risk of diabetes (40–42). Conversely, the prevalence of diabetes was found to be lower in patients with familial hypercholesterolemia compared with their unaffected relatives (43). In mice, the knockout of *ApoA1* or *ApoB1* in pancreatic β -cells was found to cause the accumulation of cellular cholesterol and impairment of glucose tolerance (15–18). Mechanistically, these findings were mainly linked to impaired β -cell function, namely insulin secretion. Cholesterol regulates the activity of glucose transporter, glucokinase, and L-type voltage-gated Ca^{2+}

channels as well as K^+ ATP channels by determining lipid rafts and membrane fluidity (44).

Several laboratories provided data indicating that overload of the ER, mitochondria, or plasma membrane with cholesterol also limits the survival of pancreatic β -cells (35). Excess cholesterol in ER membranes induces the depletion of calcium stores and subsequent ER stress and apoptosis (45). In mitochondrial membranes, excess cholesterol promotes the release of cytochrome C and hence apoptosis (46, 47). In the plasma membrane, excess cholesterol provokes the generation of reactive oxygen species, which activate apoptosis-inducing kinases such as p38 MAPK and JNK, cause mitochondrial stress, and lead to cellular apoptosis via depletion of antioxidants (48). In agreement with the damaging potential of cholesterol, we found

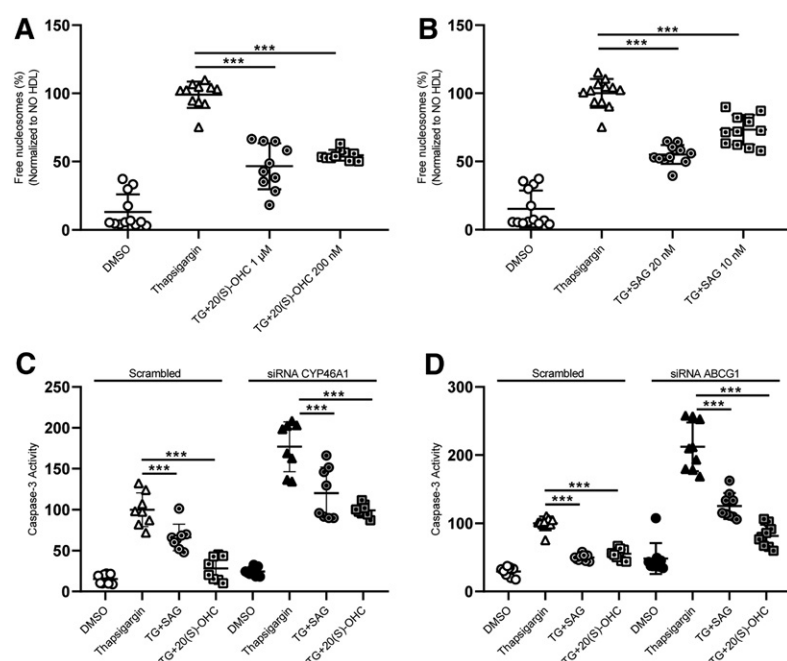


Fig. 9. The agonists of SMO rescue CYP46A1- or ABCG1-induced β -cell death. INS1e cells treated with 100 nM of TG in the presence or absence of 20(S)-OHC (A) or SAG (B) for 4 h. Cell death was recorded by using the free nucleosomes assay (A, B). INS1e cells were transfected with specific siRNA against *Cyp46a1* (C), *Abcg1* (D), or with nonsilencing siRNA (Scrambled). After 48 h of transfection, the cells were treated with 100 nM of TG in presence and absence of 20(S)-OHC or SAG for 4 h. Cell death was recorded via free caspase-3 assay (C, D). Data are presented as the mean \pm SD of three independent experiments, which were analyzed by one-way ANOVA coupled with Tukey's test for multiple comparisons in groups of Scrambled and knockdown conditions, respectively. *** $P \leq 0.001$, ** $P \leq 0.01$, * $P \leq 0.05$.

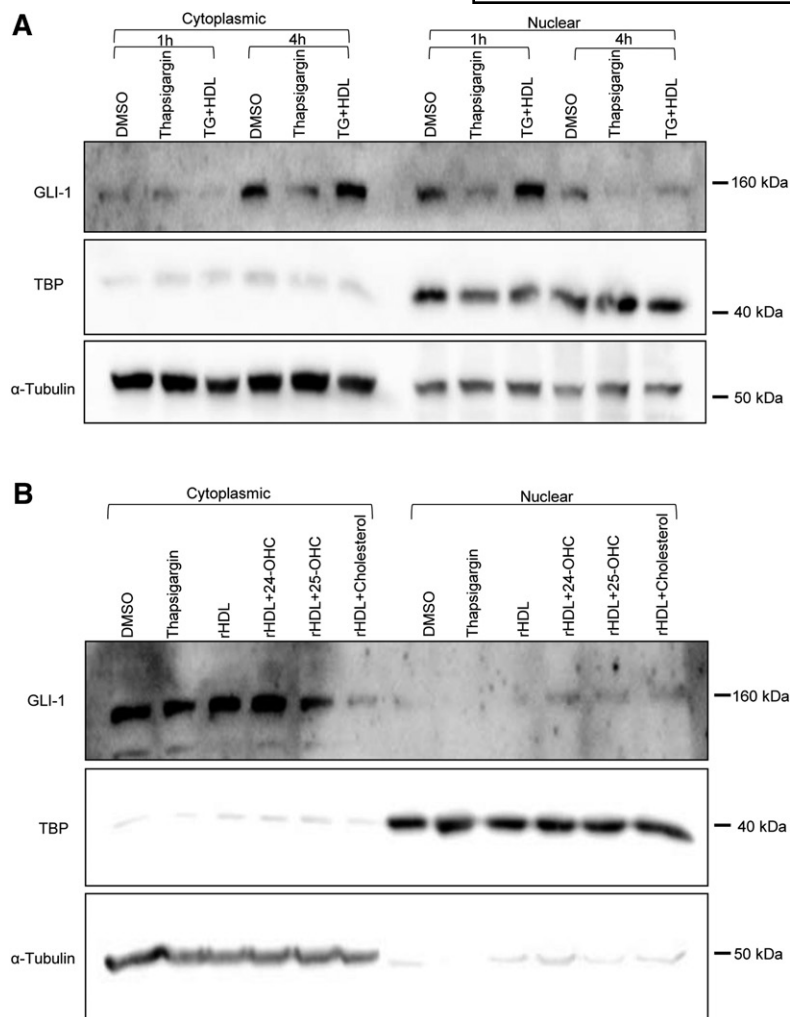


Fig. 10. Nuclear translocation of GLI-1 is inhibited by TG but promoted by native HDL and oxysterol-enriched rHDL. INS1e cells were treated with 100 nM of TG and incubated with 50 µg/ml native HDL for 1 h or 4 h (A) or with 20 µg/ml rHDL (1 apoA-I:100 DOPC:±0.01 oxysterol, molar ratio) for 4 h (B). Cells were fractionated into cytoplasmic and nuclear fractions and the fractions were immunoblotted with anti-GLI1, anti-TBP, and anti-α-tubulin.

that apoptosis increased upon knockdown of ABC transporters and was prevented by HDL-induced cholesterol efflux (Figs. 3, 7, 9). Also, in macrophages or endothelial cells, the impairment of ABCA1- or ABCG1-mediated cholesterol efflux was found to promote cell death (49, 50). However, in contrast to a damaging effect of cholesterol, in our study, the inhibition of cholesterol synthesis by statin treatment or RNA interference with *Dhcr24* boosted β-cell apoptosis significantly and inhibited the anti-apoptotic function of HDL. Also in other cell types, statin treatment was found to induce apoptosis (51–54). It thus appears that the cellular distribution, metabolism, or transport of cholesterol rather than its global cellular concentration limits the survival of INS1e cells and other cells.

Indeed, we here showed that HDL inhibits ER stress-induced apoptosis of INS1e cells by transporting and mobilizing specific oxysterols. The interference with CYP enzymes producing 24-OHC or 25-OHC elevated TG-induced apoptosis and diminished the anti-apoptotic activities of HDL and CSL-111 (Fig. 5). Even more so, also in the absence of HDL, we observed a dramatic increase in TG-induced apoptosis upon silencing of *Cyp46a1* and *Ch25h*. Conversely, the anti-apoptotic activity of rHDL was enhanced by its supplementation with 24-OHC or 25-OHC (Fig. 6). In fact, oxysterols carried not only by HDL but

also by LDL (Fig. 11) appear to lend anti-apoptotic activities to these lipoproteins

Previous studies reported both pro- and anti-apoptotic effects of 24-OHC (55–59). Possibly, the discrepant findings are due to differences in concentrations (micromolar vs. nanomolar) or the origin (endogenously produced vs. exogenously supplied) of the oxysterol in the various cell culture models. Of note, the addition of 24-OHC, 25-OHC, or cholesterol rescued the anti-apoptotic activity of rHDL more profoundly in the absence of ABCG1 than in the absence of CYP46A1 (Fig. 7A, C). Also of note, in the absence of oxysterols, rHDL was able to reduce the enhanced apoptosis upon silencing of *Ch25h* but not upon silencing of *Cyp46a1* (Fig. 7B, C). This suggests that downstream metabolites of 24-OHC are more potent inhibitors of apoptosis than 24-OHC itself. Possible candidates are di- or trihydroxylated 24-hydroxysterols or cholestenoic acids formed by CYP39A1, HSD3B7, and CYP27A1 (60).

In view of their anti-apoptotic effects, it is important to note that not only 24-OHC and 25-OHC but also 7α-OHC or 7β-OHC were more effectively effluxed by CSL-111 than cholesterol both in the presence or absence of TG, i.e., with or without ER stress (Fig. 4). In fact, CSL-111 promoted net cholesterol efflux into the medium only in the absence of the ER stress inducer TG (Fig. 4C). Also, in neuronal cells,

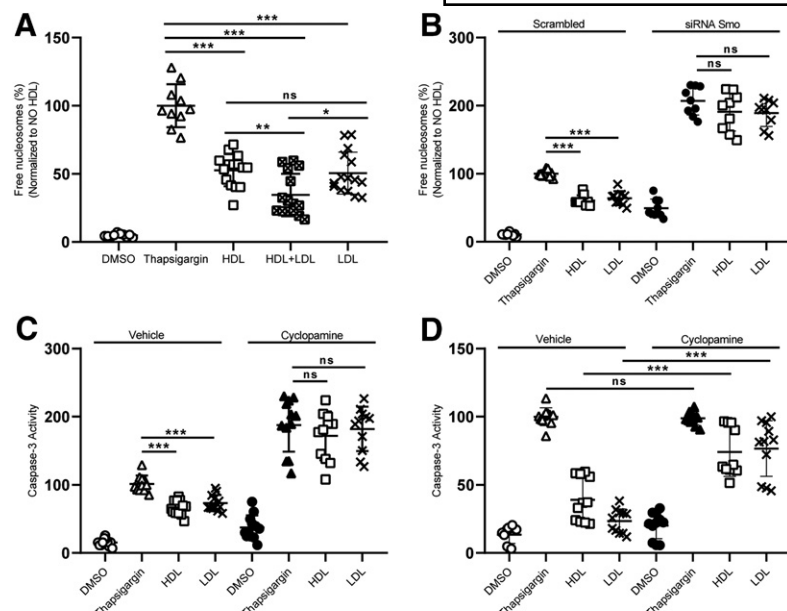


Fig. 11. Anti-apoptotic effects of LDL depend on SMO. INS1e cells were treated with 100 nM of TG for 4 h in the presence or absence of 25 μ g/ml native HDL, LDL, or both (A). INS1e cells were transfected with specific siRNA against *Smo* and nonsilencing siRNA (Scrambled) (B) or pretreated with cyclopamine for 30 min (C, D). After 48 h of transfection or cyclopamine treatment, the cells were treated with 100 nM (B, C) or 50 nM of TG (D) and incubated with HDL or LDL for 4 h (B, C) or 16 h (D). Cell death was recorded with the free nucleosomes assay (A–D). Data are presented as the mean \pm SD of three independent experiments, which were analyzed by one-way ANOVA coupled with Tukey's test for multiple comparisons. *** $P \leq 0.001$, ** $P \leq 0.01$, * $P \leq 0.05$.

24-OHC was found to be effluxed efficiently by HDL in an ABCA1-dependent manner (50). The lipid-free apoA-I did not have any effect on apoptosis in our experiments (supplemental Fig. S2); likewise, apoA-I did not mediate any efflux of 24-OHC from neuronal cells (61). Also of note, ABCG1 knockout mice showed a prominent accumulation of 24-OHC, 25-OHC, and 27-OHC in the lung tissue (51). In ABCG1-overexpressing cells, these oxysterols with hydroxyl groups at the terminal end were effluxed more efficiently than oxysterols with hydroxylated C-atoms in the ring structure (62).

Oxysterols are known to act through G protein-coupled receptors, such as G protein-coupled receptor 183 (EBI2) and SMO, or nuclear receptors, such as LXR, retinoic acid receptor-related orphan receptor, or estrogen receptor α (NR3A1) (63). LXR regulates the expression of ABC transporters like *ABCA1* and *ABCG1* (64). Treatment with an LXR agonist did not show any anti-apoptotic activity either in basal conditions or after inhibition of CYP enzymes

(supplemental Fig. S8). Thereby, we ruled out that anti-apoptotic activities of oxysterols are due to LXR activation and subsequent elevation of *Abca1* or *Abcg1* gene expression. We rather provide evidence that oxysterols contained or mobilized by HDL target the Hh signaling receptor SMO to exert anti-apoptotic signaling. Interestingly, Hh signaling was previously shown to protect β -cells from cytokine-induced toxicity by a mechanism that is activated by the Indian or Sonic Hh proteins, IHH and SHH (20). By contrast, we showed that SMO, but not its activator IHH or its inhibitor PTCH1, contributed to apoptosis protection in our ER stress-induced cell culture model. Indeed, the anti-apoptotic and ER stress-releasing activities of HDL were abrogated by both RNA interference with *Smo* and pharmacological inhibition of SMO with cyclopamine (Fig. 8) but not by interference with *Ptch1* or *Ihh* (supplemental Fig. S10). Interestingly, SMO agonists such as SAG or 20(S)-OHC significantly reduced TG-induced apoptosis and rescued cell death induced by *Cyp46a1* or

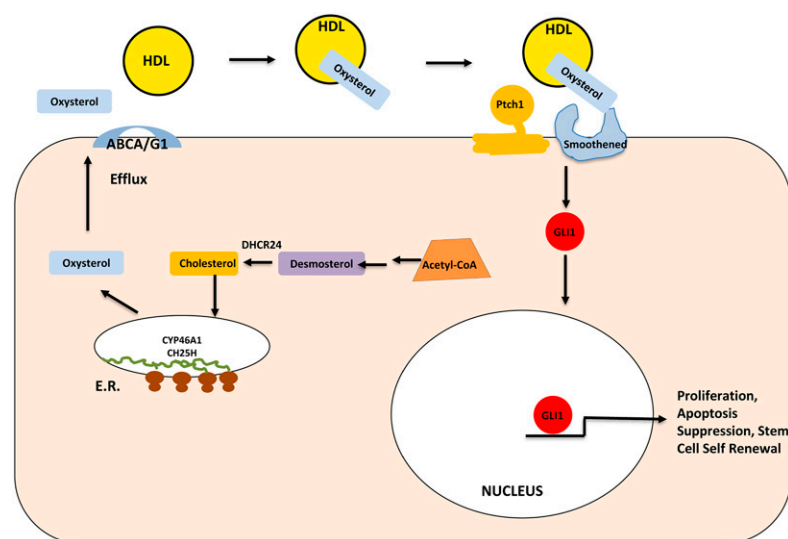



Fig. 12. The mechanism of HDL to protect pancreatic β -cells from TG-induced ER stress and apoptosis.

Abcg1 interference similar to oxysterol supplementation of rHDL (Fig. 9). Also in agreement with the involvement of Hh signaling in the anti-apoptotic effects of HDL, the translocation of GLI-1, i.e., the transcription factor activated by SMO, into the nucleus (65) was decreased by ER stress but restored by both native HDL and rHDL supplemented with oxysterols (Fig. 10).

Our study does not definitely resolve the mechanism by which oxysterols contained or mobilized by lipoproteins regulate SMO activity and thereby prevent ER stress-induced apoptosis. In general, sterols have been described to regulate Hh signaling by two distinct mechanisms (66). On the one hand, oxysterols directly activate SMO. On the other hand, lateral distribution of sterols in the plasma membrane was found to be crucial for the relative activity of SMO and its inhibitor PTCH1. Cholesterol or specific oxysterols such as 20-OHC, 24-OHC, and 25-OHC, but not 7 β -OHC and 19-OHC, are required for Hh signaling through SMO in medulloblastoma cells (67–69). The effects of 20-OHC were shown to be stereoselective and to synergize with the allosteric agonist SAG (70). The site of hydroxylation on the cholesterol backbone correlates with oxysterol activity. Activating oxysterols are hydroxylated on the flexible cholesterol chain, whereas nonactivating ones, such as 7- and 19-OHC, are hydroxylated on the four-ring core of cholesterol (67). In accordance with this specificity, in our hands the supplementation with 7 α -OHC or 7 β -OHC did not enhance the ability of rHDL to inhibit TG-induced apoptosis (supplemental Fig. S6). In addition to direct binding of oxysterols to the cysteine-rich domain of SMO (71), it was also reported that cholesterol is an endogenous activator of Hh signaling, driving a conformational change of SMO (37). Depending on the distribution of cholesterol between the inner and outer leaflets of the plasma membrane, either SMO or its inhibitor PTCH1 are more active (19). Because ABC transporters including ABCA1 and ABCG1 are floppases (72), we cannot rule out that HDL, LDL, or ABC transporters modulate Hh signaling by modulating the distribution of cholesterol between the leaflets of the plasma membrane. However, this will not explain the specific effects of 24-OHC and CYP46A1 on ER stress and apoptosis.

In conclusion, we have here shown a novel interaction between HDL-mediated sterol mobilization and Hh signaling. Our findings are limited by the use of an artificial cell culture system and a nonphysiological stimulus of ER stress and apoptosis. Hence, it will be important to test whether this mechanism is also operative upon provocation of ER stress by more physiological stimuli in primary cells and, ultimately, in vivo. If so, the crucial role of HDL in sterol efflux as well as the ubiquitous abundance of Hh signaling and its multiple cellular processes, such as differentiation, raise the question of whether other cellular activities of HDL involve modulation of Hh signaling. With respect to diabetes, it will be interesting to see whether transdifferentiation of islet-cells into β -cells (73) is modulated by HDL. 

We thank Dr. Samuel Wright (CSL Behring, USA) for providing CSL-111.

1. Cho, J. H., J. W. Kim, J. A. Shin, J. Shin, and K. H. Yoon. 2011. β -Cell mass in people with type 2 diabetes. *J. Diabetes Investig.* **2**: 6–17.
2. Eizirik, D. L., A. K. Cardozo, and M. Cnop. 2008. The role for endoplasmic reticulum stress in diabetes mellitus. *Endocr. Rev.* **29**: 42–61.
3. Oyadomari, S., E. Araki, and M. Mori. 2002. Endoplasmic reticulum stress-mediated apoptosis in pancreatic beta-cells. *Apoptosis*. **7**: 335–345.
4. Cnop, M., N. Welsh, J. C. Jonas, A. Jorns, S. Lenzen, and D. L. Eizirik. 2005. Mechanisms of pancreatic beta-cell death in type 1 and type 2 diabetes: many differences, few similarities. *Diabetes*. **54** (Suppl. 2): S97–S107.
5. Elouil, H., M. Bensellam, Y. Guiot, D. Vander Mierde, S. M. Pascal, F. C. Schuit, and J. C. Jonas. 2007. Acute nutrient regulation of the unfolded protein response and integrated stress response in cultured rat pancreatic islets. *Diabetologia*. **50**: 1442–1452.
6. Papa, F. R. 2012. Endoplasmic reticulum stress, pancreatic beta-cell degeneration, and diabetes. *Cold Spring Harb. Perspect. Med.* **2**: a007666.
7. von Eckardstein, A., and C. Widmann. 2014. High-density lipoprotein, beta cells, and diabetes. *Cardiovasc. Res.* **103**: 384–394.
8. Holmes, M. V., M. Ala-Korpela, and G. D. Smith. 2017. Mendelian randomization in cardiometabolic disease: challenges in evaluating causality. *Nat. Rev. Cardiol.* **14**: 577–590.
9. Li, N., J. Fu, D. P. Koonen, J. A. Kuivenhoven, H. Snieder, and M. H. Hofker. 2014. Are hypertriglyceridemia and low HDL causal factors in the development of insulin resistance? *Atherosclerosis*. **233**: 130–138.
10. Parhofer, K. G. 2015. Interaction between glucose and lipid metabolism: more than diabetic dyslipidemia. *Diabetes Metab. J.* **39**: 353–362.
11. Annema, W., and A. von Eckardstein. 2016. Dysfunctional high-density lipoproteins in coronary heart disease: implications for diagnostics and therapy. *Transl. Res.* **173**: 30–57.
12. Nofer, J. R. 2015. Signal transduction by HDL: agonists, receptors, and signaling cascades. *Handb. Exp. Pharmacol.* **224**: 229–256.
13. Sorci-Thomas, M. G., and M. J. Thomas. 2016. Microdomains, inflammation, and atherosclerosis. *Circ. Res.* **118**: 679–691.
14. Maxwell, K. N., R. E. Soccio, E. M. Duncan, E. Sehayek, and J. L. Breslow. 2003. Novel putative SREBP and LXR target genes identified by microarray analysis in liver of cholesterol-fed mice. *J. Lipid Res.* **44**: 2109–2119.
15. Brunham, L. R., J. K. Kruit, T. D. Pape, J. M. Timmins, A. Q. Reuwer, Z. Vasanji, B. J. Marsh, B. Rodrigues, J. D. Johnson, J. S. Parks, et al. 2007. Beta-cell ABCA1 influences insulin secretion, glucose homeostasis and response to thiazolidinedione treatment. *Nat. Med.* **13**: 340–347.
16. Sturek, J. M., J. D. Castle, A. P. Trace, L. C. Page, A. M. Castle, C. Evans-Molina, J. S. Parks, R. G. Mirmira, and C. C. Hedrick. 2010. An intracellular role for ABCG1-mediated cholesterol transport in the regulated secretory pathway of mouse pancreatic beta cells. *J. Clin. Invest.* **120**: 2575–2589.
17. Kruit, J. K., N. Wijesekara, C. Westwell-Roper, T. Vanmierlo, W. de Haan, A. Bhattacharjee, R. Tang, C. L. Wellington, D. Lütjohann, J. D. Johnson, et al. 2012. Loss of both ABCA1 and ABCG1 results in increased disturbances in islet sterol homeostasis, inflammation, and impaired beta-cell function. *Diabetes*. **61**: 659–664.
18. Kruit, J. K., P. H. Kremer, L. Dai, R. Tang, P. Ruddle, W. de Haan, L. R. Brunham, C. B. Verchere, and M. R. Hayden. 2010. Cholesterol efflux via ATP-binding cassette transporter A1 (ABCA1) and cholesterol uptake via the LDL receptor influences cholesterol-induced impairment of beta cell function in mice. *Diabetologia*. **53**: 1110–1119.
19. Zhang, Y., D. P. Bulkley, Y. Xin, K. J. Roberts, D. E. Asanow, A. Sharma, B. R. Myers, W. Cho, Y. Cheng, and P. A. Beachy. 2018. Structural basis for cholesterol transport-like activity of the Hedgehog receptor Patched. *Cell*. **175**: 1352–1364.
20. Umeda, H., N. Ozaki, N. Mizutani, T. Fukuyama, H. Nagasaki, H. Arima, and Y. Oiso. 2010. Protective effect of hedgehog signaling on cytokine-induced cytotoxicity in pancreatic beta-cells. *Exp. Clin. Endocrinol. Diabetes*. **118**: 692–698.
21. Kieser, E., S. Swierczynski, C. Mayr, T. Jager, J. Schmidt, D. Neureiter, T. Kiesslich, and R. Illig. 2016. Differential role of Hedgehog signaling in human pancreatic (patho-) physiology: An up to date review. *World J. Gastrointest. Pathophysiol.* **7**: 199–210.
22. Drew, B. G., S. J. Duffy, M. F. Formosa, A. K. Natoli, D. C. Henstridge, S. A. Penfold, W. G. Thomas, N. Mukhamedova, B. de Courten, J. M.

- Forbes, et al. 2009. High-density lipoprotein modulates glucose metabolism in patients with type 2 diabetes mellitus. *Circulation*. **119**: 2103–2111.
23. Sambrook, J. F. 1990. The involvement of calcium in transport of secretory proteins from the endoplasmic reticulum. *Cell*. **61**: 197–199.
 24. Pétremand, J., J. Puyal, J. Y. Chatton, J. Duprez, F. Allagnat, M. Frias, R. W. James, G. Waeber, J. C. Jonas, and C. Widmann. 2012. HDLs protect pancreatic beta-cells against ER stress by restoring protein folding and trafficking. *Diabetes*. **61**: 1100–1111.
 25. Briscoe, J., and P. P. Therond. 2013. The mechanisms of Hedgehog signalling and its roles in development and disease. *Nat. Rev. Mol. Cell Biol.* **14**: 416–429.
 26. Merglen, A., S. Theander, B. Rubi, G. Chaffard, C. B. Wollheim, and P. Maechler. 2004. Glucose sensitivity and metabolism-secretion coupling studied during two-year continuous culture in INS-1E insulinoma cells. *Endocrinology*. **145**: 667–678.
 27. Janjic, D., P. Maechler, N. Sekine, C. Bartley, A. S. Annen, and C. B. Wollheim. 1999. Free radical modulation of insulin release in INS-1 cells exposed to alloxan. *Biochem. Pharmacol.* **57**: 639–648.
 28. Camus, M. C., M. J. Chapman, P. Forgez, and P. M. Laplaud. 1983. Distribution and characterization of the serum lipoproteins and apoproteins in the mouse, *Mus musculus*. *J. Lipid Res.* **24**: 1210–1228.
 29. Rohrer, L., C. Cavelier, S. Fuchs, M. A. Schluter, W. Volker, and A. von Eckardstein. 2006. Binding, internalization and transport of apolipoprotein A-I by vascular endothelial cells. *Biochim. Biophys. Acta*. **1761**: 186–194.
 30. Ohnsorg, P. M., L. Rohrer, D. Perisa, A. Kateifides, A. Chroni, D. Kardassios, V. I. Zannis, and A. von Eckardstein. 2011. Carboxyl terminus of apolipoprotein A-I (ApoA-I) is necessary for the transport of lipid-free ApoA-I but not prelipidated ApoA-I particles through aortic endothelial cells. *J. Biol. Chem.* **286**: 7744–7754.
 31. Riwanto, M., L. Rohrer, B. Roschitzki, C. Besler, P. Mocharla, M. Mueller, D. Perisa, K. Heinrich, L. Altwegg, A. von Eckardstein, et al. 2013. Altered activation of endothelial anti- and proapoptotic pathways by high-density lipoprotein from patients with coronary artery disease: role of high-density lipoprotein-proteome remodeling. *Circulation*. **127**: 891–904.
 32. Sutter, I., S. Velagapudi, A. Othman, M. Riwanto, J. Manz, L. Rohrer, K. Rentsch, T. Hornemann, U. Landmesser, and A. von Eckardstein. 2015. Plasmalogens of high-density lipoproteins (HDL) are associated with coronary artery disease and anti-apoptotic activity of HDL. *Atherosclerosis*. **241**: 539–546.
 33. Zheng, K. H., and E. S. Stroes. 2016. HDL infusion for the management of atherosclerosis: current developments and new directions. *Curr. Opin. Lipidol.* **27**: 592–596.
 34. Tricoci, P., D. M. D'Andrea, P. A. Gurbel, Z. Yao, M. Cuchel, B. Winston, R. Schott, R. Weiss, M. A. Blazing, L. Cannon, et al. 2015. Infusion of reconstituted high-density lipoprotein, CSL112, in patients with atherosclerosis: safety and pharmacokinetic results from a phase 2a randomized clinical trial. *J. Am. Heart Assoc.* **4**: e002171.
 35. Mackay, D. S., P. J. Jones, S. B. Myrie, J. Plat, and D. Lutjohann. 2014. Methodological considerations for the harmonization of non-cholesterol sterol bio-analysis. *J. Chromatogr. B Analyt. Technol. Biomed. Life Sci.* **957**: 116–122.
 36. Šošić-Jurjević, B., D. Lutjohann, K. Renko, B. Filipovic, N. Radulovic, V. Ajdzanovic, S. Trifunovic, N. Nestorovic, J. Zivanovic, M. Manojlovic Stojanowski, et al. 2019. The isoflavones genistein and daidzein increase hepatic concentration of thyroid hormones and affect cholesterol metabolism in middle-aged male rats. *J. Steroid Biochem. Mol. Biol.* **190**: 1–10.
 37. Huang, P., D. Nedelcu, M. Watanabe, C. Jao, Y. Kim, J. Liu, and A. Salic. 2016. Cellular cholesterol directly activates Smoothed Hedgehog signaling. *Cell*. **166**: 1176–1187.
 38. Burkard, I., A. von Eckardstein, G. Waeber, P. Vollenweider, and K. M. Rentsch. 2007. Lipoprotein distribution and biological variation of 24S- and 27-hydroxycholesterol in healthy volunteers. *Atherosclerosis*. **194**: 71–78.
 39. Babiker, A., and U. Diczfalusy. 1998. Transport of side-chain oxidized oxysterols in the human circulation. *Biochim. Biophys. Acta*. **1392**: 333–339.
 40. Sattar, N., D. Preiss, H. M. Murray, P. Welsh, B. M. Buckley, A. J. de Craen, S. R. Seshasai, J. J. McMurray, D. J. Freeman, J. W. Jukema, et al. 2010. Statins and risk of incident diabetes: a collaborative meta-analysis of randomised statin trials. *Lancet*. **375**: 735–742.
 41. Preiss, D., S. R. Seshasai, P. Welsh, S. A. Murphy, J. E. Ho, D. D. Waters, D. A. DeMicco, P. Barter, C. P. Cannon, M. S. Sabatine, et al. 2011. Risk of incident diabetes with intensive-dose compared with moderate-dose statin therapy: a meta-analysis. *JAMA*. **305**: 2556–2564.
 42. Ference, B. A., J. G. Robinson, R. D. Brook, A. L. Catapano, M. J. Chapman, D. R. Neff, S. Voros, R. P. Giugliano, G. Davey Smith, S. Fazio, et al. 2016. Variation in PCSK9 and HMGCR and risk of cardiovascular disease and diabetes. *N. Engl. J. Med.* **375**: 2144–2153.
 43. Besseling, J., J. J. Kastelein, J. C. Defesche, B. A. Hutten, and G. K. Hovingh. 2015. Association between familial hypercholesterolemia and prevalence of type 2 diabetes mellitus. *JAMA*. **313**: 1029–1036.
 44. Perego, C., L. Da Dalt, A. Pirillo, A. Galli, A. L. Catapano, and G. D. Norata. 2019. Cholesterol metabolism, pancreatic beta-cell function and diabetes. *Biochim. Biophys. Acta Mol. Basis Dis.* **1865**: 2149–2156.
 45. Kong, F. J., J. H. Wu, S. Y. Sun, and J. Q. Zhou. 2017. The endoplasmic reticulum stress/autophagy pathway is involved in cholesterol-induced pancreatic beta-cell injury. *Sci. Rep.* **7**: 44746.
 46. Carrasco-Pozo, C., K. N. Tan, M. Reyes-Farias, N. De La Jara, S. T. Ngo, D. F. Garcia-Diaz, P. Llanos, M. J. Cires, and K. Borges. 2016. The deleterious effect of cholesterol and protection by quercetin on mitochondrial bioenergetics of pancreatic beta-cells, glycemic control and inflammation: In vitro and in vivo studies. *Redox Biol.* **9**: 229–243.
 47. Zhao, Y. F., L. Wang, S. Lee, Q. Sun, Y. Tuo, Y. Wang, J. Pei, and C. Chen. 2010. Cholesterol induces mitochondrial dysfunction and apoptosis in mouse pancreatic beta-cell line MIN6 cells. *Endocrine*. **37**: 76–82.
 48. Lu, X., J. Liu, F. Hou, Z. Liu, X. Cao, H. Seo, and B. Gao. 2011. Cholesterol induces pancreatic beta cell apoptosis through oxidative stress pathway. *Cell Stress Chaperones*. **16**: 539–548.
 49. Yvan-Charvet, L., T. A. Pagler, T. A. Seimon, E. Thorp, C. L. Welch, J. L. Witztum, I. Tabas, and A. R. Tall. 2010. ABCA1 and ABCG1 protect against oxidative stress-induced macrophage apoptosis during efferocytosis. *Circ. Res.* **106**: 1861–1869.
 50. Xue, J., J. Wei, X. Dong, C. Zhu, Y. Li, A. Song, and Z. Liu. 2013. ABCG1 deficiency promotes endothelial apoptosis by endoplasmic reticulum stress-dependent pathway. *J. Physiol. Sci.* **63**: 435–444.
 51. Li, L. Z., M. Zhao, L. Zhang, J. He, T. F. Zhang, J. B. Guo, L. Yu, J. Zhao, X. Y. Yuan, and S. Q. Peng. 2019. Atorvastatin induces mitochondrial dysfunction and cell apoptosis in HepG2 cells via inhibition of the Nrf2 pathway. *J. Appl. Toxicol.* **39**: 1394–1404.
 52. Sheikhholeslami, K., A. Ali Sher, S. Lockman, D. Kroft, M. Ganjibakhsh, K. Nejati-Koshki, S. Shojaei, S. Ghavami, and M. Rastegar. 2019. Simvastatin induces apoptosis in medulloblastoma brain tumor cells via mevalonate cascade prenylation substrates. *Cancers (Basel)*. **11**: doi:10.3390/cancers11070994.
 53. Ma, Q., Y. Gao, P. Xu, K. Li, X. Xu, J. Gao, Y. Qi, J. Xu, Y. Yang, W. Song, et al. 2019. Atorvastatin inhibits breast cancer cells by down-regulating PTEN/AKT pathway via promoting ras homolog family member B (RhoB). *BioMed Res. Int.* **2019**: 3235021.
 54. Kim, W. H., C. H. Lee, J. H. Han, S. Kim, S. Y. Kim, J. H. Lim, K. M. Park, D. S. Shin, and C. H. Woo. 2019. C/EBP homologous protein deficiency inhibits statin-induced myotoxicity. *Biochem. Biophys. Res. Commun.* **508**: 857–863.
 55. Petrov, A. M., N. Mast, Y. Li, and I. A. Pikuleva. 2019. The key genes, phosphoproteins, processes, and pathways affected by efavirenz-activated CYP46A1 in the amyloid-decreasing paradigm of efavirenz treatment. *FASEB J.* **33**: 8782–8798.
 56. Nakazawa, T., Y. Miyanoki, Y. Urano, M. Uehara, Y. Saito, and N. Noguchi. 2017. Effect of vitamin E on 24(S)-hydroxycholesterol-induced necroptosis-like cell death and apoptosis. *J. Steroid Biochem. Mol. Biol.* **169**: 69–76.
 57. Yamanaka, K., Y. Urano, W. Takabe, Y. Saito, and N. Noguchi. 2014. Induction of apoptosis and necroptosis by 24(S)-hydroxycholesterol is dependent on activity of acyl-CoA:cholesterol acyltransferase 1. *Cell Death Dis.* **5**: e990.
 58. Okabe, A., Y. Urano, S. Itoh, N. Suda, R. Kotani, Y. Nishimura, Y. Saito, and N. Noguchi. 2013. Adaptive responses induced by 24S-hydroxycholesterol through liver X receptor pathway reduce 7-ketocholesterol-caused neuronal cell death. *Redox Biol.* **2**: 28–35.
 59. Emanuelsson, I., and M. Norlin. 2012. Protective effects of 27- and 24-hydroxycholesterol against staurosporine-induced cell death in undifferentiated neuroblastoma SH-SY5Y cells. *Neurosci. Lett.* **525**: 44–48.
 60. Crick, P. J., E. Yutuc, J. Abdel-Khalik, A. Saeed, C. Betsholtz, G. Genove, I. Bjorkhem, Y. Wang, and W. J. Griffiths. 2019. Formation

and metabolism of oxysterols and cholestenic acids found in the mouse circulation: Lessons learnt from deuterium-enrichment experiments and the CYP46A1 transgenic mouse. *J. Steroid Biochem. Mol. Biol.* **195**: 105475.

61. Matsuda, A., K. Nagao, M. Matsuo, N. Kioka, and K. Ueda. 2013. 24(S)-hydroxycholesterol is actively eliminated from neuronal cells by ABCA1. *J. Neurochem.* **126**: 93–101.
62. Engel, T., M. Fobker, J. Buchmann, F. Kannenberg, S. Rust, J. R. Nofer, A. Schurmann, and U. Seedorf. 2014. 3beta,5alpha,6beta-Cholestanetriol and 25-hydroxycholesterol accumulate in ATP-binding cassette transporter G1 (ABCG1)-deficiency. *Atherosclerosis*. **235**: 122–129.
63. Mutemberezi, V., O. Guillemot-Legris, and G. G. Muccioli. 2016. Oxysterols: from cholesterol metabolites to key mediators. *Prog. Lipid Res.* **64**: 152–169.
64. Hong, C., and P. Tontonoz. 2014. Liver X receptors in lipid metabolism: opportunities for drug discovery. *Nat. Rev. Drug Discov.* **13**: 433–444.
65. Kong, J. H., C. Siebold, and R. Rohatgi. 2019. Biochemical mechanisms of vertebrate hedgehog signaling. *Development*. **146**: doi:10.1242/dev.166892.
66. Hu, A., and B. L. Song. 2019. The interplay of Patched, Smoothened and cholesterol in Hedgehog signaling. *Curr. Opin. Cell Biol.* **61**: 31–38.
67. Corcoran, R. B., and M. P. Scott. 2006. Oxysterols stimulate Sonic hedgehog signal transduction and proliferation of medulloblastoma cells. *Proc. Natl. Acad. Sci. USA*. **103**: 8408–8413.
68. Dwyer, J. R., N. Sever, M. Carlson, S. F. Nelson, P. A. Beachy, and F. Parhami. 2007. Oxysterols are novel activators of the hedgehog signaling pathway in pluripotent mesenchymal cells. *J. Biol. Chem.* **282**: 8959–8968.
69. Nedelcu, D., J. Liu, Y. Xu, C. Jao, and A. Salic. 2013. Oxysterol binding to the extracellular domain of Smoothened in Hedgehog signaling. *Nat. Chem. Biol.* **9**: 557–564.
70. Nachtergaele, S., L. K. Mydock, K. Krishnan, J. Rammohan, P. H. Schlesinger, D. F. Covey, and R. Rohatgi. 2012. Oxysterols are allosteric activators of the oncoprotein Smoothened. *Nat. Chem. Biol.* **8**: 211–220.
71. Nachtergaele, S., D. M. Whalen, L. K. Mydock, Z. Zhao, T. Malinauskas, K. Krishnan, P. W. Ingham, D. F. Covey, C. Siebold, and R. Rohatgi. 2013. Structure and function of the Smoothened extracellular domain in vertebrate Hedgehog signaling. *eLife*. **2**: e01340.
72. Gulshan, K., G. Brubaker, S. Wang, S. L. Hazen, and J. D. Smith. 2013. Sphingomyelin depletion impairs anionic phospholipid inward translocation and induces cholesterol efflux. *J. Biol. Chem.* **288**: 37166–37179.
73. Swisa, A., B. Glaser, and Y. Dor. 2017. Metabolic stress and compromised identity of pancreatic beta cells. *Front. Genet.* **8**: 21.